Radiology

Intrabiliary RF Heat-enhanced Local Chemotherapy of a Cholangiocarcinoma Cell Line: Monitoring with Dual-Modality Imaging—Preclinical Study[1]

Feng Zhang, MD, PhD
Thomas Le, MD
Xia Wu, MD, PhD[2]
Han Wang, MD, PhD
Tong Zhang, MD, PhD
Yanfeng Meng, MD, PhD
Baojie Wei, MD, PhD
Stephanie S. Soriano, MD
Patrick Willis, BS
Orpheus Kolokythas, MD
Xiaoming Yang, MD, PhD

Purpose: To determine whether magnetic resonance (MR) imaging heating guidewire–mediated radiofrequency (RF) hyperthermia could enhance the therapeutic effect of gemcitabine and 5-fluorouracil (5-FU) in a cholangiocarcinoma cell line and local deposit doses of chemotherapeutic drugs in swine common bile duct (CBD) walls.

Materials and Methods: The animal protocol was approved by the institutional animal care and use committee. Green fluorescent protein–labeled human cholangiocarcinoma cells and cholangiocarcinomas in 24 mice were treated with *(a)* combination therapy with chemotherapy (gemcitabine and 5-FU) plus RF hyperthermia, *(b)* chemotherapy only, *(c)* RF hyperthermia only, or *(d)* phosphate-buffered saline. Cell proliferation was quantified, and tumor changes over time were monitored with 14.0-T MR imaging and optical imaging. To enable further validation of technical feasibility, intrabiliary local delivery of gemcitabine and 5-FU was performed by using a microporous balloon with (eight pigs) or without (eight pigs) RF hyperthermia. Chemotherapy deposit doses in the bile duct walls were quantified by means of high-pressure liquid chromatography. The nonparametric Mann-Whitney *U* test and the paired-sample Wilcoxon signed rank test were used for data analysis.

Results: Combination therapy induced lower mean levels of cell proliferation than chemotherapy only and RF hyperthermia only (0.39 ± 0.13 [standard deviation] vs 0.87 ± 0.10 and 1.03 ± 0.13, $P < .001$). Combination therapy resulted in smaller relative tumor volume than chemotherapy only and RF hyperthermia only (0.65 ± 0.03 vs 1.30 ± 0.021 and 1.37 ± 0.05, $P = .001$). Only in the combination therapy group did both MR imaging and optical imaging show substantial decreases in apparent diffusion coefficients and fluorescent signals in tumor masses immediately after the treatments. Chemotherapy quantification showed a higher average drug deposit dose in swine CBD walls with intrabiliary RF hyperthermia than without it (gemcitabine: 0.32 mg/g of tissue ± 0.033 vs 0.260 mg/g ± 0.030 and 5-FU: 0.660 mg/g ± 0.060 vs 0.52 mg/g ± 0.050, $P < .05$).

Conclusion: The use of intrabiliary MR imaging heating guidewire–mediated RF hyperthermia can enhance the chemotherapeutic effect on a human cholangiocarcinoma cell line and local drug deposition in swine CBD tissues.

[1] From the Image-Guided Bio-Molecular Intervention Research and Section of Vascular & Interventional Radiology, Department of Radiology, Institute for Stem Cell and Regenerative Medicine, University of Washington School of Medicine, 850 Republican St, Seattle, WA 98109. Received May 15, 2013; revision requested June 24; revision received July 21; accepted August 6; final version accepted August 14. **Address correspondence to** X.Y. (e-mail: *xmyang@u.washington.edu*).

[2] **Current address:** Department of Radiology, Sir Run Run Shaw Hospital, Zhejiang University School of Medicine, Hangzhou, China.

Patients with biliary malignancies have poor prognoses. Unfortunately, by the time such malignancies are diagnosed, they are usually unresectable. However, for the minority of patients who have resectable tumors, surgical treatment is often associated with substantial postoperative morbidity and mortality (1,2).

Systemic chemotherapy remains the mainstay of palliative treatment for these patients (3). Adjuvant chemotherapy with gemcitabine and 5-fluorouracil (5-FU) has been the first-line therapy for patients with unresectable biliary tract cancers (4). However, the benefits of systemic chemotherapy are limited by its nonspecific delivery, which results in lower than needed drug doses for the targeted tumors and causes systemic toxicities to other organs. Intrabiliary local therapies, such as photodynamic therapy or intraluminal low-dose-rate iridium 192 brachytherapy combined with biliary stent placement, have been used in an attempt to treat patients with unresectable extrahepatic bile duct carcinoma (5,6), but the overall benefits of these approaches are not clear as of now. Recent investigations (7–10) have focused on the application of thermal energy to enhance chemotherapy for a variety of malignancies. For cholangiocarcinoma, thermal chemotherapy is achieved by means of either whole-body hyperthermia or external hyperthermia around the liver (11,12). Because of the deep anatomic location of a bile cancer, it is difficult to generate highly focused hyperthermia at the target tumor by using systemic or external hyperthermia.

Over the past decade, one of the achievements in the field of magnetic resonance (MR) imaging is the development of intraluminal MR imaging and MR imaging-guided interventions (13). Among these new techniques is the application of an intraluminal MR imaging–radiofrequency (RF) heat system, with the key component being a Food and Drug Administration–approved MR imaging heating guidewire. The MR imaging heating guidewire has three major functions, acting as *(a)* an intraluminal MR receiver antenna for generating high-spatial-resolution MR imaging of luminal walls (14,15), *(b)* a conventional guidewire for guiding intraluminal interventional procedure (16,17), and *(c)* an intraluminal RF hyperthermia source for enhancing gene delivery (18). This "three-in-one" function of simultaneous imaging, guiding, and heating may provide an opportunity to solve the current clinical problems in the management of biliary malignancies. Therefore, the purpose of our study was to determine whether MR imaging heating guidewire–mediated RF hyperthermia could enhance the therapeutic effect of gemcitabine and 5-FU in a cholangiocarcinoma cell line and local deposit doses of chemotherapeutic drugs in swine common bile duct (CBD) walls.

Advances in Knowledge

- Combination therapy with MR imaging heating guidewire–mediated radiofrequency (RF) hyperthermia and chemotherapy induced the lowest cell proliferation and relative tumor volume compared with those after chemotherapy only and RF hyperthermia only.
- Only in the group treated with combination therapy did diffusion-weighted MR images show decreased apparent diffusion coefficients (ADCs) at day 1 and increased ADCs at day 7 and day 14 after the treatment; optical imaging findings also showed decreased fluorescent signal intensity in the group treated with combination therapy.
- RF hyperthermia can enhance the deposition of gemcitabine and 5-fluorouracil (5-FU) in swine common bile duct (CBD) walls, as compared with chemotherapy without RF hyperthermia ($P < .05$).

Implication for Patient Care

- The findings of our study indicate that RF hyperthermia can enhance the chemotherapeutic effect of gemcitabine and 5-FU in a cholangiocarcinoma cell line and local drug deposition in CBD tissues, which may pose a potential clinical application for managing bile duct cancer.

Materials and Methods

Study Design

Our study was divided into three distinct phases: *(a)* an in vitro experiment to confirm RF hyperthermia–enhanced chemotherapeutic effects on cells from a human cholangiocarcinoma cell line, *(b)* an in vivo experiment on mice to validate the feasibility of using diffusion-weighted (DW) MR imaging and optical imaging to monitor the response of cholangiocarcinoma to RF hyperthermia–enhanced chemotherapy, and *(c)* an in vivo experiment in swine to establish the proof of principle that intrabiliary MR imaging heating guidewire–mediated RF hyperthermia could enhance local chemotherapeutic drug deposition in bile duct walls.

Published online before print
10.1148/radiol.13130866 **Content codes:** GI MI IR

Radiology 2014; 270:400–408

Abbreviations:
ADC = apparent diffusion coefficient
CBD = common bile duct
DW = diffusion weighted
5-FU = 5-fluorouracil
GFP = green fluorescent protein
PBS = phosphate-buffered saline
RF = radiofrequency
RSI = relative signal intensity
TUNEL = terminal deoxynucleotidyl transferase dUTP nick end labeling

Author contributions:
Guarantors of integrity of entire study, F.Z., X.W., T.Z., X.Y.; study concepts/study design or data acquisition or data analysis/interpretation, all authors; manuscript drafting or manuscript revision for important intellectual content, all authors; manuscript final version approval, all authors; literature research, F.Z., T.L., X.W., B.W.; clinical studies, X.W., P.W.; experimental studies, F.Z., T.L., X.W., H.W., T.Z., Y.M., B.W., S.S.S.; statistical analysis, F.Z., T.L., X.W., B.W.; and manuscript editing, F.Z., T.L., X.W., B.W., S.S.S., P.W., O.K., X.Y.

Funding:
This research was supported by the National Institutes of Health (grant RO1EB012467).

Conflicts of interest are listed at the end of this article.

See also Science to Practice in this issue.

In Vitro Experiments

Cell culture and RF hyperthermia–enhanced chemotherapy.—Human cholangiocarcinoma cells (MZ-ChA-1) (16) were transfected by eGFP (enhanced green fluorescent protein [GFP]) lentiviral particles (Lentifect; GeneCopoeia, Rockville, Md) according to the protocol provided by the manufacturer to create GFP-positive cells. GFP-positive cells were sorted out by using a fluorescence-activated cell sorting technique (Aria II; Becton Dickinson, Franklin Lakes, NJ). Cells (2×10^5) were seeded in each chamber of the four-chamber cell culture slides (Nalge Nunc International, Rochester, NY) and were maintained in Delbecco's modified Eagle's medium supplemented with 10% fetal bovine serum (Mediatech, Manassas, Va) for further experiments. RF hyperthermia was performed as described in the literature (18). The treatments were initiated when the cell confluence reached 80%. Cells in different groups were treated with *(a)* combination therapy of 101 μM gemcitabine (Eli Lilly, Indianapolis, Ind) and 95 μM 5-FU (APP Pharmaceuticals, Schaumburg, Ill) with 30 minutes of RF hyperthermia at a temperature between 41.7°C and 42.5°C, *(b)* 30 minutes of RF hyperthermia only, *(c)* gemcitabine (101 μM) plus 5-FU (95 μM) without RF hyperthermia, and *(d)* phosphate-buffered saline (PBS) to serve as a control. We used the half maximal inhibitory concentration (IC_{50}) doses of gemcitabine and 5-FU for cell treatment, both of which have substantial killing effect on this cell line (19).

Cell proliferation assay.—Combination therapy was performed by adding gemcitabine and 5-FU to the medium and heating the cells at the temperature between 41.7°C and 42.5°C with RF power at 12–14 W for 30 minutes (20). Gemcitabine and 5-FU were kept in the medium for 24 hours after RF hyperthermia. Cells in the chemotherapy-only group were treated with gemcitabine and 5-FU for the same duration (24 hours). Cell proliferation was evaluated with the MTS assay (3-(4,5-dimethylthiazol-2-yl)-5-(3-carboxymethoxyphenyl)-2-(4-sulfophenyl)-2H-tetrazolium) (Promega, Madison, Wis). The absorbance was detected at 490 nm with a microplate reader (VersaMax; Molecular Devices, Sunnyvale, Calif). Relative cell proliferations of different cell groups were evaluated by using the equation $A_{treated}/A_{control}$, where A is absorbance. Cells on the slide were subsequently counterstained with 4',6-diamidino-2-phenylindole (DAPI; Vector Laboratories, Burlingame, Calif) and were then imaged with a laser confocal microscope (A1R; Nikon, Tokyo, Japan). All the experiments for each of the cell groups were repeated six times (X.W., a research fellow with 5 years of experience in cell and animal experimentation).

In Vivo Experiments in Mice

Animal model.—The animal protocol was approved by the institutional animal care and use committee. Cholangiocarcinoma tumor xenografts were created in 24 nu/nu mice aged 4–6 weeks (Charles River Laboratories, Wilmington, Mass) by means of subcutaneous inoculation of 5×10^6 to 1×10^7 GFP-positive cells in 80 μL PBS into the left side of the back of each mouse (X.W. and F.Z., with 5 years of experience in animal experiments). The sizes of the tumors reached 5–10 mm in diameter within 28 days. During the entire procedure, the animal was anesthetized with 1%–3% isoflurane (Piramal Healthcare, Andhra Pradesh, India) in 100% oxygen.

RF hyperthermia and chemotherapy.—Mice with tumors were randomly allocated to four groups. Six mice in each group were treated with *(a)* combination therapy, with intratumoral injection of 25 mg gemcitabine per kilogram of body weight and 25 mg/kg 5-FU in 100 μL PBS followed by RF hyperthermia at a temperature between 41.7°C and 42.5°C for 30 minutes; *(b)* 30 minutes of RF hyperthermia only; *(c)* intratumoral injection of 25 mg/kg gemcitabine and 25 mg/kg 5-FU only; and *(d)* intratumoral injection of 100 μL PBS to serve as a control (F.Z. and X.W., radiologic research scientists; and T.L., a 4th-year radiology resident). RF hyperthermia was performed by inserting a 0.022-inch MR imaging heating guidewire into the tumor with its hyperthermia source at the center of the tumor. A 400-μm fiberoptic temperature probe (PhotonControl, Burnaby, British Columbia, Canada) was subcutaneously placed in parallel to the MR imaging heating guidewire at the margin of the tumor (Fig 1, *A*). By adjusting RF output power at around 10 W, the temperature was kept between 41.7°C and 42.5°C in the tumor mass.

MR imaging.—MR imaging was performed by using a 14-T vertical wide-bore MR spectrometer and a microimaging coil (Bruker, Billerica, Mass). T2-weighted imaging and DW imaging were used to image the tumors 1 day prior to and 1, 7, and 14 days after the treatment. Axial and sagittal T2-weighted imaging was performed by using a respiratory-gated rapid acquisition with relaxation enhancement (RARE) sequence. Parameters were as follows: repetition time msec/echo time msec, 890/4.5; field of view, 2.56 cm; matrix, 128 × 128; section thickness, 1 mm, without gap; number of signals acquired, four; RARE factor, eight; and refocusing flip angle, 180°. Axial DW imaging was then performed by using a respiratory-gated spin-echo sequence at three *b* values (25, 586, and 1112 sec/mm^2) with the following parameters: 3000/27.5; field of view, 2.56 cm; matrix, 256 × 128; section thickness, 1 mm, without gap; number of signals acquired, three; and flip angle, 90°.

GFP-based optical imaging.—The optical imaging system consisted of a charge-coupled device camera cooled to −20°C (SensiCam; Cooke, Romulus, Mich) mounted on a light-tight specimen chamber (dark box), an external excitation light source, and a Windows-based computer system. Mice were imaged 1 day prior to and 1, 7, and 14 days after treatment. During image acquisition, the mice were placed in the prone position. The GFP-positive tumors were excited by the external light source with a mean selected wavelength at 475 nm ± 20 (standard deviation) for a 1-second exposure time, while the emission light from the tumor mass was collected by using a filter with its wavelength at 500 nm ± 20. The electronic output of the camera was routed to the computer for image storage, display, and analysis.

Figure 1

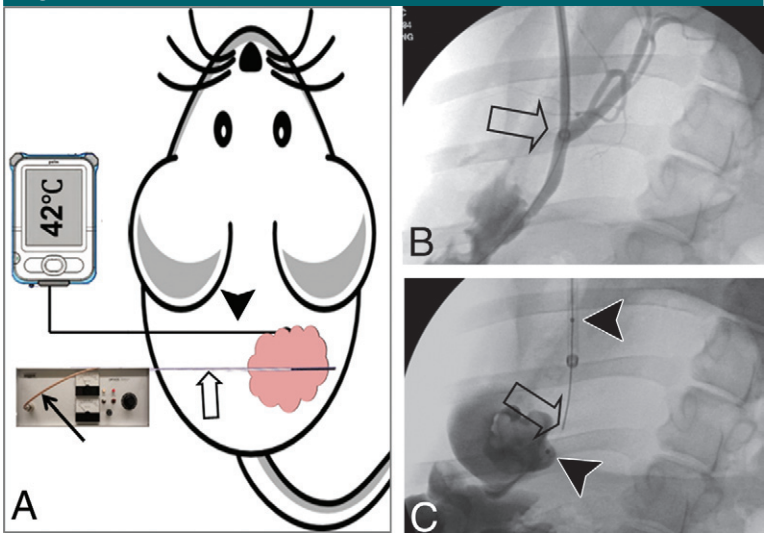

Figure 1: RF hyperthermia treatment of mouse cholangiocarcinoma and swine CBD. *A,* A 0.022-inch RF hyperthermia wire (open arrow) is placed in the center of the tumor, which is connected to the RF generator by a cable (solid arrow), while a fiberoptic temperature probe (arrowhead) is percutaneously placed at the margin of the tumor to instantly measure the temperature. *B,* X-ray fluoroscopic image shows the 10-F introducer (arrow) placed in the CBD of a pig. *C,* An RF hyperthermia wire (arrow) was positioned within a microporous agent delivery balloon (arrowheads = the two markers of the balloon).

Image analysis.—For measurement of apparent diffusion coefficient (ADC) (F.Z., with 10 years of MR imaging experience), the image section with the largest tumor diameter was selected for generating ADC maps and measuring ADC. A freehand region of interest (ROI) was placed over the tumor mass, encompassing the entire cross-sectional area of the tumor. The pre- and posttreatment ROIs were drawn at the same section to reduce variability. ADC was calculated by using ImageJ software (National Institutes of Health, Bethesda, Md). For the tumor volume measurement (F.Z.), tumor volume in cubic millimeters was calculated on the basis of axial T2-weighted images. The tumor border was delineated manually, and the area was automatically calculated by using ImageJ. Given the irregular contour and shape of the tumors, the tumor volume V was calculated according to the following equation: $V = s \cdot (a_1 + a_2 + a_3 + \ldots + a_n)$, where s is the section interval and a_1 through a_n are the areas of sections (21). Relative tumor volume (RTV) at different time points for each tumor was calculated (X.W.) by using the following equation: $RTV = TV_{Dn}/TV_{D0,}$ where TV is tumor volume, D_n represents day 1, day 7, or day 14 after treatment, and D_0 is the day before treatment. For optical imaging, freehand ROIs were manually placed to encompass the GFP-positive tumor masses by using ImageJ, with which signal intensities were measured (F.Z.). To keep the consistency while measuring the signal intensities, for each tumor mass at different time points the ROI was copied from the pretreatment image onto the same tumor mass on the posttreatment images. Relative signal intensity (RSI) was obtained by using the equation $RSI = SI_{tumor}/SI_{background}$.

In Vivo Experiments in Pigs

Animals.—Pig experiments were approved by the institutional animal care and use committee. Sixteen domestic pigs, 40–50 kg in weight, were sedated by means of intramuscular injection of Telazol at 4.4 mg/kg and xylazine at 1 mg/kg (both drugs manufactured by Fort Dodge Animal Health, Fort Dodge, Iowa) and were then mechanically ventilated with 1%–3% isoflurane in 100% oxygen.

Catheterization of CBDs.—Through a subcostal laparotomy, the gallbladder was mobilized and lifted out of the peritoneal cavity. With fluoroscopic guidance, a 10-F introducer was advanced, through the gallbladder and the cystic duct, into the CBD over a 0.035-inch hydrophilic guidewire (Terumo, Tokyo, Japan) (Fig 1, *B*). A 1.1-mm fiberoptic temperature probe was attached to a 6 × 40-mm balloon catheter (Ultra-thin SDS; Boston Scientific, Natick, Mass), and the 0.022-inch MR imaging heating guidewire was inserted into the guidewire channel of the balloon catheter (Fig 1, *C*), which was placed in the target CBD through the introducer. The abdominal incision was closed with sutures, and the introducer was secured to the skin (F.Z., X.W., Y.M., H.W., T.Z., B.W.).

Intrabiliary chemotherapeutic drug delivery and RF hyperthermia.—For the animal group with combination therapy of both chemotherapy and RF hyperthermia (n = 8), the MR imaging heating guidewire was connected to the custom RF generator, and the heating was initiated with an output power of 10 W, which was monitored by the fiberoptic temperature probe. When the temperature reached 42°C, a mixture of 100 mg 5-FU and 50 mg gemcitabine in 10 mL PBS was delivered into the CBD wall by using a microporous balloon at an infusion rate of 0.5 mL/sec. After the delivery of the drugs, the temperature was maintained at 42°C for an additional 30 minutes. For the study group treated with chemotherapy infusion only (n = 8), after the same amounts of drugs were delivered into the CBD wall, the balloon was kept in the target CBD for 30 minutes. After the drug delivery, animals were euthanized for quantification of deposit drug doses within the CBD walls.

Histologic Examination

For mice, tumors were harvested 14 days after treatments. Tumor tissues were cryosliced at 10 μm for apoptosis staining. The level of apoptosis on

Figure 2

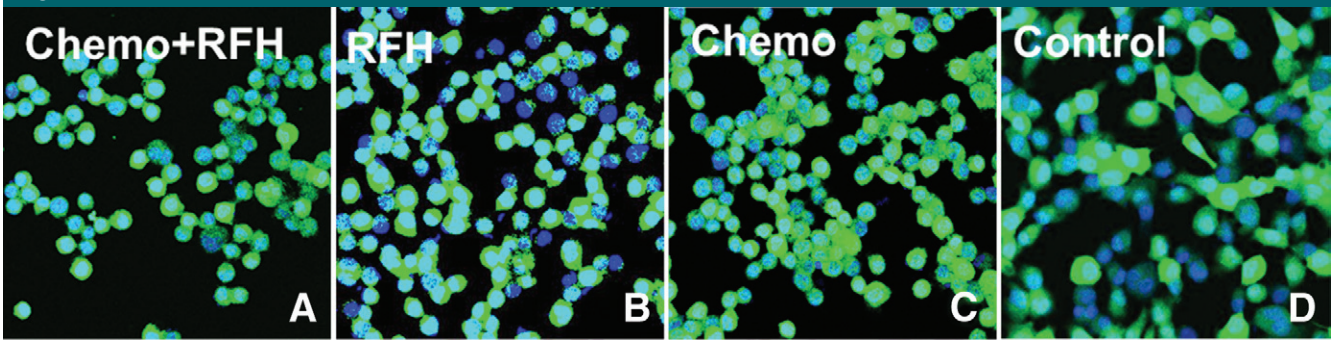

Figure 2: *A–D,* Confocal microscopic images show that the number of viable cells in the combination therapy group (*Chemo+RFH* = chemotherapy and RF hyperthermia) decreased remarkably compared with that in the other three groups.

each slide was determined with a terminal deoxynucleotidyl transferase dUTP nick end labeling assay (TUNEL) by using a TACS XL Blue Label kit, according to the protocol provided by the manufacturer (Trivegen, Gaithersburg, Md). Cells with dark blue dots in the cytoplasm were recognized as apoptotic cells. On each slide, six high-power fields were pictured randomly by using a digital camera (DP72; Olympus, Tokyo, Japan). Results are expressed as the apoptotic index (AI), which was calculated by using the following equation: $AI = N_{AC}/N_{CF} \cdot 100\%$, where N_{AC} is the number of apoptotic cells and N_{CF} is the number of cells in the field.

Drug Quantification

For drug quantification in pig CBD tissues, after drug delivery, CBDs were harvested, weighed, and then homogenized in 5 mL PBS by using a tissue grinder (PYREX Ten Broeck, Corning, Corning, NY). Gemcitabine and 5-FU were extracted, reconstituted in 200-μL mobile phase (water/methanol = 90/10), and analyzed by using high-pressure liquid chromatography (Waters, Milford, Mass). Briefly, 20-μL solutions were injected into a 5-μm, 250 × 4.6-mm column (C18; Phenomenex, Torrance, Calif), eluted by a mobile phase at a flow rate of 1 mL/min, and monitored at 254 nm by means of ultraviolet light absorption. The calibration curves were created for each drug by using standard solutions ranging from 0.1 to 500 μg/mL. Linear regression analysis was performed by plotting the peak areas *(y)* of each drug against the respective concentrations *(x)*. Regression correlation coefficients of the lineal curve were greater than 0.990.

Statistical Analysis

Statistical software (SPSS, version 19.0; SPSS, Chicago, Ill) was used for all data analysis. The nonparametric Mann-Whitney *U* test was used to compare *(a)* relative proliferation rates between cell groups, *(b)* relative tumor volumes at day 14 after treatment between mouse groups, and *(c)* deposit doses of 5-FU and gemcitabine in swine CBDs between the group with RF heating and that without. The paired-sample Wilcoxon signed rank test was used to compare the ADCs and signal intensities of GFP fluorescence at different time points within the same group. $P < .05$ was considered to indicate a significant difference.

Results

Therapeutic Effect on Cells

The in vitro experiments showed that RF hyperthermia could enhance the cell-killing effect of gemcitabine and 5-FU. Confocal microscopy showed that combination therapy (chemotherapy plus RF hyperthermia) killed many more cancer cells than the chemotherapy-only and RF hyperthermia–only treatments (Fig 2). The killing effect was more severe in the cell group with combination therapy at 42°C than in the cell groups at 37°C and 40°C (relative proliferation: 0.39 ± 0.13 vs 0.87 ± 0.10, $P < .001$; and 0.39 ± 0.13 vs 0.73 ± 0.15, $P = .001$). Compared with findings in the cell group treated with RF hyperthermia only, combination therapy at 42°C significantly reduced cell proliferation (0.39 ± 0.13 vs 1.03 ± 0.13, $P < .001$).

Therapeutic Effect on Mice Tumors

The in vivo experiments on mice showed that the combination therapy significantly inhibited the growth of tumors (Fig 3). The average relative tumor volume for each group at different time points is illustrated in Figure 4, *A*. Fourteen days after the treatment, the average relative tumor volume was the smallest in the combination therapy group, as compared with volumes in the chemotherapy-only group (0.65 ± 0.03 vs 1.30 ± 0.021, $P = .001$) and the RF hyperthermia–only group (0.65 ± 0.03 vs 1.37 ± 0.05, $P = .001$). A trend to difference in relative tumor volume was seen between the chemotherapy-only and RF hyperthermia–only groups ($P = .055$). The chemotherapy-only treatment did not inhibit tumor growth, as compared with growth in the control group ($P = .65$).

Image Analysis

Regarding the ADCs in the four groups, 1 day after the treatment, only the average ADC in the combination therapy group significantly decreased compared with those in the pretreatment,

Figure 3

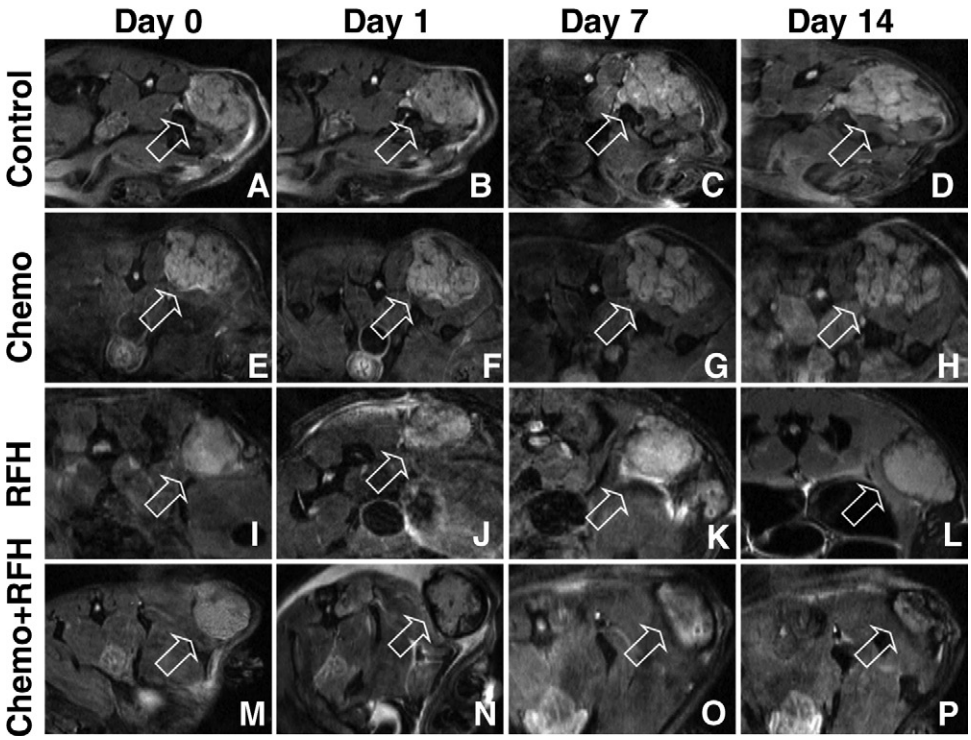

Figure 3: *A–P,* Axial DW MR images of mice cholangiocarcinoma masses (arrow) in four animal groups with different treatments: *A–D,* control; *E–H,* chemotherapy only; *I–L,* RF hyperthermia *(RFH)* only; and, *M–P,* combination therapy. The size of the tumor treated with combination therapy decreased 14 days after the treatment, while the sizes of the tumors increased in the control, chemotherapy-only, and RF hyperthermia–only groups.

chemotherapy-only, RF hyperthermia–only, and control groups. Seven and 14 days after treatment, the average ADC in the combination therapy group increased compared with that before treatment *(*$P < .001$ for both comparisons*)* (Fig 4, *B*). Quantitative analysis of the RSIs of fluorescence in different groups showed that the RSIs of tumors in the combination therapy group significantly decreased from day 1 through day 14 after treatment ($P < .001$), while the RSIs in the three control groups either increased or stayed at the same levels over the follow-up period (Fig 5).

Histologic Examination

Histologic analysis of tumor apoptosis showed a higher apoptotic index in the group treated with combination therapy than in the groups treated with RF hyperthermia only or chemotherapy only (37.3% ± 5.8% vs 11.8% ± 1.9%, $P = .02$; and 37.3% ± 5.8% vs 6.4% ± 2.1%, $P = .007$) (Fig 6).

Drug Quantification

The in vivo experiments in pigs showed higher deposit doses of chemotherapeutic drugs in the CBD walls treated with intrabiliary RF hyperthermia than in those treated without RF hyperthermia (gemcitabine: 0.32 mg/g of tissue ± 0.033 vs 0.260 mg/g of tissue ± 0.030, $P = .013$; and 5-FU: 0.660 mg/g of tissue ± 0.060 vs 0.52 mg/g of tissue ± 0.050, $P = .024$).

Discussion

The findings of our study show that RF hyperthermia can enhance the killing effect of gemcitabine and 5-FU on the human cholangiocarcinoma cell line, as manifested by shrunken tumor volumes, decreased ADCs 1 day after treatment, increased ADCs 7 and 14 days after treatment, and diminished fluorescent signal intensities of tumors. Our study in pigs also confirmed that *(a)* it is feasible to locally deliver gemcitabine and 5-FU into CBD walls, and *(b)* RF hyperthermia can enhance the local deposition of gemcitabine and 5-FU in CBD walls.

To create localized substantial hyperthermia in a target biliary tumor is a challenging task. An external alternating-current magnetic field has been applied to create localized hyperthermia in mouse tumors in which docetaxel-embedded magnetoliposomes (DMLs) were injected (22), but the feasibility of this technique for treating deep-seated bile duct cancer needs to be investigated. We used the MR imaging heating guidewire to create localized hyperthermia in cholangiocarcinoma xenografts in mice and in target CBD walls in pigs

Figure 4

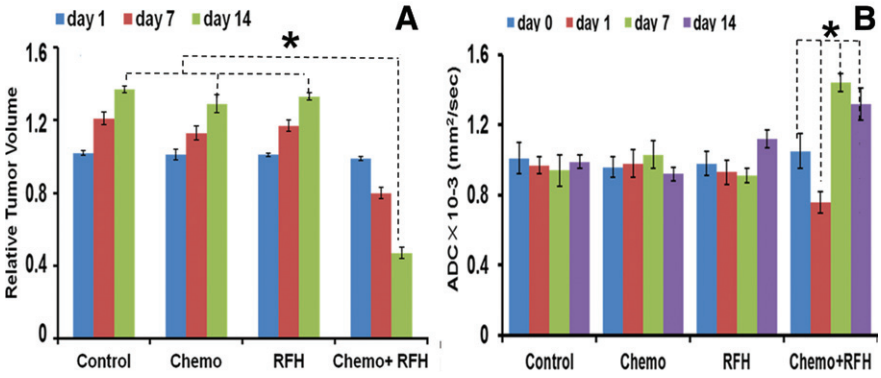

Figure 4: *A,* Bar graph shows average relative tumor volume in each group at different time points. Fourteen days after the treatment, the average relative tumor volume was the smallest in the combination therapy group, as compared with those in the other groups (*$P = .001$). *B,* Bar graph shows average ADCs in four animal groups treated with various therapies. The combination therapy group shows decreased ADCs at day 1 and increased ADCs at days 7 and 14 after treatment (*$P < .001$). *RFH* = RF hyperthermia.

Figure 5

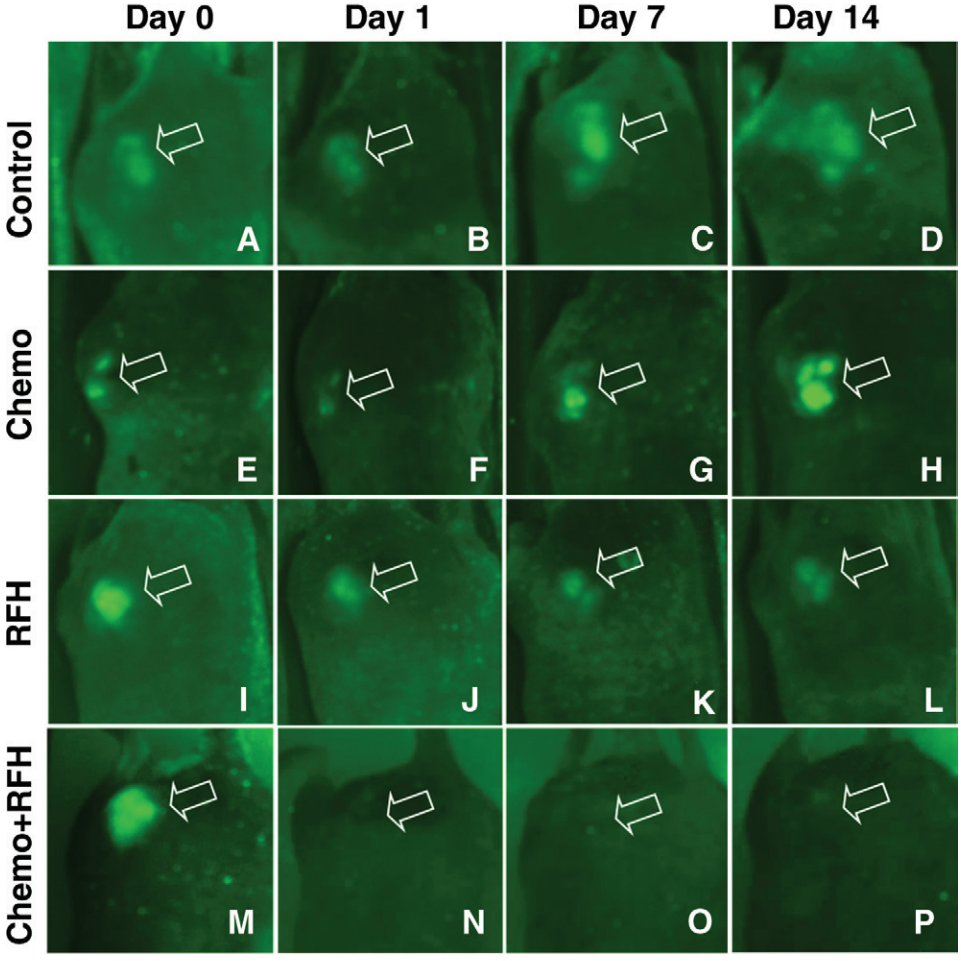

Figure 5: *A–P,* Optical images of GFP-labeled cholangiocarcinoma masses (arrow) in mice in different treatment groups. In, *A–D,* the control mouse and, *E–H,* the mouse treated with chemotherapy only, the tumor sizes and fluorescent signals increased over the 14-day follow-up period. In, *I–L,* the mouse treated with RF hyperthermia *(RFH)* only, the fluorescent signal slightly decreased at day 1 and then remained visible through day 14, while in, *M–P,* the mouse treated with combination therapy, the fluorescent signals were barely seen from day 1 through day 14 after treatment.

Figure 6

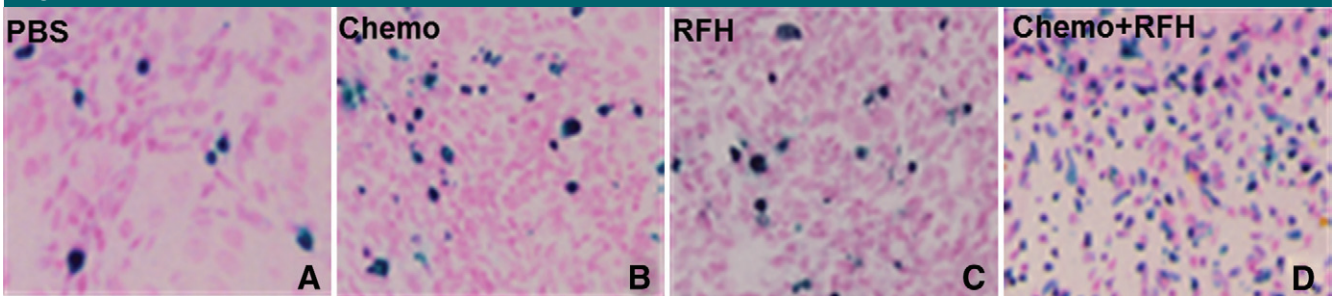

Figure 6: *A–D,* Histologic images of tumor cell apoptosis after the therapies. TUNEL staining of tumors collected at day 14 shows more apoptotic cells (as blue spots) in, *D,* the cell group treated with combination therapy than in the other three groups (original magnification, ×200).

to enhance chemotherapy, thus providing substantial localized therapeutic hyperthermia. The temperature we used is within the clinically relevant temperature range (40°C–45°C) (20). The biologic basis of hyperthermia-enhanced chemotherapy is perhaps associated with the mechanisms that hyperthermia can reverse chemotherapy resistance, increase oxygen radical production, and facilitate drug penetration and therefore uptake by cancer cells (7,10). Previous work (23) has revealed the potential usefulness of combining RF ablation with intravenous long-circulating temperature-sensitive liposomal doxorubicin to improve tumor growth control and decrease viable tumor. Increased drug deposition has also been observed, particularly in the tumor tissue surrounding the primary ablation zone (24).

Conventional criteria for clinical evaluation of therapeutic response in cancers are based on the Response Evaluation Criteria in Solid Tumors (RECIST) guidelines. However, the RECIST guidelines lack the ability to predict the early response of cancers to therapy (25,26). In our study, we observed significant phenomena, including decreased ADCs 1 day after the treatment, increased ADCs 7 and 14 days after the treatment, and diminished fluorescent signal intensities of tumors over the follow-up period. This finding may indicate the usefulness of both DW MR imaging and fluorescent optical imaging in monitoring the early response of cholangiocarcinomas to RF hyperthermia–enhanced chemotherapeutic effects.

DW MR imaging is a functional imaging technique that measures the mobility of water molecules in tissues. The dense cellularity of a cancer mass has limited diffusion capability, which is reflected as a low ADC. This parameter is very useful for characterizing tumors and quantifying treatment-induced changes, which occur earlier than morphologic or volumetric alterations (27). The underlying pathophysiologic mechanism for the instant decrease in ADC 1 day after combination chemotherapy may be related to cytotoxicity-induced intracellular edema, which lessens the extracellular space and thereby restricts the diffusion of water molecules. The increase in the ADC of target tumors 7 and 14 days after treatment can be explained by the RF hyperthermia–enhanced cytotoxic effect, which leads to overall cell loss and a reduction in cell density and therefore to an associated increase in the extracellular space that results in more freedom for the water molecules.

In our study, GFP-based optical imaging also displayed the early molecular and biologic changes in tumors 1 day after RF hyperthermia–enhanced chemotherapy. The advantages of this optical imaging technique include its low cost, high sensitivity, and noninvasive and real-time depiction of the biologic events in tumors (28). However, the main weaknesses of optical imaging, which limit its clinical applications, are the poor tissue penetration of fluorescent lights and the low spatial resolution of the targets (28,29). Developing molecular imaging techniques for interventional therapies may address this issue for translation of optical imaging from preclinical applications in small animals to clinical practice in humans (30).

Our study had limitations. We used a hyperthermia temperature of 42.0°C only. Additional experiments are warranted to select the optimal temperature and to maximize the enhancing effect of RF hyperthermia on chemotherapy. Further studies on different types of chemotherapy, doses, and hyperthermia regimens are needed to compare the appropriate combination therapy of RF hyperthermia with chemotherapeutic drugs for bile duct cancer. Because our study focused on establishing the proof of principle of the technique, we did not investigate the deposit doses of drugs in cholangiocarcinoma cells or tumors at different time points after hyperthermia, and the numbers of samples were small, but this had no impact on the inference of statistical significance. We used only one dose of the chemotherapeutic drugs in treating mouse tumors and in validating the technique of intrabiliary RF hyperthermia–enhanced drug delivery into swine CBD walls. We need to perform a series of survival studies in swine to select the dosage that can be tolerated by the normal bile duct tissue. In addition, because currently no large-animal models with cholangiocarcinomas exist, we were unable to perform a preclinical validation study of this technology by means of serial survival experiments with large-animal tumor models.

In conclusion, our study results confirm that the use of intrabiliary MR imaging heating guidewire–mediated RF hyperthermia can enhance chemotherapeutic effects on a human cholangiocarcinoma cell line and on local drug deposition in swine CBD tissues.

Practical application: This technique of intrabiliary RF hyperthermia–enhanced chemotherapy may be translated into the clinical setting to manage unresectable bile duct cancers.

Disclosures of Conflicts of Interest: F.Z. No relevant conflicts of interest to disclose. **T.L.** No relevant conflicts of interest to disclose. **X.W.** No relevant conflicts of interest to disclose. **H.W.** No relevant conflicts of interest to disclose. **T.Z.** No relevant conflicts of interest to disclose. **Y.M.** No relevant conflicts of interest to disclose. **B.W.** No relevant conflicts of interest to disclose. **S.S.S.** No relevant conflicts of interest to disclose. **P.W.** No relevant conflicts of interest to disclose. **O.K.** No relevant conflicts of interest to disclose. **X.Y.** No relevant conflicts of interest to disclose.

References

1. van Delden OM, Laméris JS. Percutaneous drainage and stenting for palliation of malignant bile duct obstruction. Eur Radiol 2008;18(3):448–456.
2. Donelli G, Guaglianone E, Di Rosa R, Fiocca F, Basoli A. Plastic biliary stent occlusion: factors involved and possible preventive approaches. Clin Med Res 2007;5(1):53–60.
3. Valle J, Wasan H, Palmer DH, et al. Cisplatin plus gemcitabine versus gemcitabine for biliary tract cancer. N Engl J Med 2010;362(14):1273–1281.
4. Pracht M, Le Roux G, Sulpice L, et al. Chemotherapy for inoperable advanced or metastatic cholangiocarcinoma: retrospective analysis of 78 cases in a single center over four years. Chemotherapy 2012;58(2):134–141.
5. Takamura A, Saito H, Kamada T, et al. Intraluminal low-dose-rate 192Ir brachytherapy combined with external beam radiotherapy and biliary stenting for unresectable extrahepatic bile duct carcinoma. Int J Radiat Oncol Biol Phys 2003;57(5):1357–1365.
6. Witzigmann H, Berr F, Ringel U, et al. Surgical and palliative management and outcome in 184 patients with hilar cholangiocarcinoma: palliative photodynamic therapy plus stenting is comparable to r1/r2 resection. Ann Surg 2006;244(2):230–239.
7. Bakshandeh-Bath A, Stoltz AS, Homann N, Wagner T, Stölting S, Peters SO. Preclinical and clinical aspects of carboplatin and gemcitabine combined with whole-body hyperthermia for pancreatic adenocarcinoma. Anticancer Res 2009;29(8):3069–3077.
8. Kouloulias VE, Dardoufas CE, Kouvaris JR, et al. Liposomal doxorubicin in conjunction with reirradiation and local hyperthermia treatment in recurrent breast cancer: a phase I/II trial. Clin Cancer Res 2002;8(2):374–382.
9. Maluta S, Schaffer M, Pioli F, et al. Regional hyperthermia combined with chemoradiotherapy in primary or recurrent locally advanced pancreatic cancer: an open-label comparative cohort trial. Strahlenther Onkol 2011;187(10):619–625.
10. Ohguri T, Imada H, Yahara K, et al. Concurrent chemoradiotherapy with gemcitabine plus regional hyperthermia for locally advanced pancreatic carcinoma: initial experience. Radiat Med 2008;26(10):587–596.
11. Kamisawa T, Tu Y, Egawa N, et al. Thermo-chemo-radiotherapy for advanced bile duct carcinoma. World J Gastroenterol 2005;11(27):4206–4209.
12. Mambrini A, Del Freo A, Pacetti P, et al. Intra-arterial and systemic chemotherapy plus external hyperthermia in unresectable biliary cancer. Clin Oncol (R Coll Radiol) 2007;19(10):805–806.
13. Yang X, Atalar E, Zerhouni EA. Intravascular MR imaging and intravascular MR-guided interventions. Int J Cardiovasc Intervent 1999;2(2):85–96.
14. Ocali O, Atalar E. Intravascular magnetic resonance imaging using a loopless catheter antenna. Magn Reson Med 1997;37(1):112–118.
15. Yang X, Atalar E, Li D, et al. Magnetic resonance imaging permits in vivo monitoring of catheter-based vascular gene delivery. Circulation 2001;104(14):1588–1590.
16. Zhang F, Li J, Meng Y, et al. Development of an intrabiliary MR imaging-monitored local agent delivery technique: a feasibility study in pigs. Radiology 2012;262(3):846–852.
17. Yang X, Atalar E. Intravascular MR imaging-guided balloon angioplasty with an MR imaging guide wire: feasibility study in rabbits. Radiology 2000;217(2):501–506.
18. Du X, Qiu B, Zhan X, et al. Radiofrequency-enhanced vascular gene transduction and expression for intravascular MR imaging-guided therapy: feasibility study in pigs. Radiology 2005;236(3):939–944.
19. Frampton GA, Lazcano EA, Li H, Mohamad A, DeMorrow S. Resveratrol enhances the sensitivity of cholangiocarcinoma to chemotherapeutic agents. Lab Invest 2010;90(9):1325–1338.
20. Partanen A, Yarmolenko PS, Viitala A, et al. Mild hyperthermia with magnetic resonance-guided high-intensity focused ultrasound for applications in drug delivery. Int J Hyperthermia 2012;28(4):320–336.
21. Dudeck O, Zeile M, Pink D, et al. Diffusion-weighted magnetic resonance imaging allows monitoring of anticancer treatment effects in patients with soft-tissue sarcomas. J Magn Reson Imaging 2008;27(5):1109–1113.
22. Yoshida M, Sato M, Yamamoto Y, et al. Tumor local chemohyperthermia using docetaxel-embedded magnetoliposomes: Interaction of chemotherapy and hyperthermia. J Gastroenterol Hepatol 2012;27(2):406–411.
23. Soundararajan A, Dodd GD 3rd, Bao A, et al. Chemoradionuclide therapy with 186Re-labeled liposomal doxorubicin in combination with radiofrequency ablation for effective treatment of head and neck cancer in a nude rat tumor xenograft model. Radiology 2011;261(3):813–823.
24. Head HW, Dodd GD 3rd, Bao A, et al. Combination radiofrequency ablation and intravenous radiolabeled liposomal doxorubicin: imaging and quantification of increased drug delivery to tumors. Radiology 2010;255(2):405–414.
25. Sala E, Kataoka MY, Priest AN, et al. Advanced ovarian cancer: multiparametric MR imaging demonstrates response- and metastasis-specific effects. Radiology 2012;263(1):149–159.
26. Ohno Y, Koyama H, Yoshikawa T, et al. Diffusion-weighted MRI versus 18F-FDG PET/CT: performance as predictors of tumor treatment response and patient survival in patients with non-small cell lung cancer receiving chemoradiotherapy. AJR Am J Roentgenol 2012;198(1):75–82.
27. Yabuuchi H, Hatakenaka M, Takayama K, et al. Non-small cell lung cancer: detection of early response to chemotherapy by using contrast-enhanced dynamic and diffusion-weighted MR imaging. Radiology 2011;261(2):598–604.
28. Ray P, Wu AM, Gambhir SS. Optical bioluminescence and positron emission tomography imaging of a novel fusion reporter gene in tumor xenografts of living mice. Cancer Res 2003;63(6):1160–1165.
29. Li C, Penet MF, Winnard P Jr, Artemov D, Bhujwalla ZM. Image-guided enzyme/prodrug cancer therapy. Clin Cancer Res 2008;14(2):515–522.
30. Yang X. Interventional molecular imaging. Radiology 2010;254(3):651–654.